A Focused Ultrasoft X-Ray Microbeam for Targeting Cells Individually with Submicrometer Accuracy

M. Folkard,[a,1] G. Schettino,[a] B. Vojnovic,[a] S. Gilchrist,[a] A. G. Michette,[b] S. J. Pfauntsch,[b] K. M. Prise[a] and B. D. Michael[a]

[a] *Gray Cancer Institute, P.O. Box 100, Mount Vernon Hospital, Northwood, Middlesex, HA6 2JR, United Kingdom; and* [b] *King's College London, Strand, London, WC2R 2LS, United Kingdom*

Folkard, M., Schettino, G., Vojnovic, B., Gilchrist, S., Michette, A. G., Pfauntsch, S. J., Prise, K. M. and Michael, B. D. A Focused Ultrasoft X-Ray Microbeam for Targeting Cells Individually with Submicrometer Accuracy. *Radiat. Res.* 156, 796–804 (2001).

The application of microbeams is providing new insights into the actions of radiation at the cell and tissue levels. So far, this has been achieved exclusively through the use of collimated charged particles. One alternative is to use ultrasoft X rays, focused by X-ray diffractive optics. We have developed a unique facility that uses 0.2–0.8-mm-diameter zone plates to focus ultrasoft X rays to a beam of less than 1 μm diameter. The zone plate images characteristic K-shell X rays of carbon or aluminum, generated by focusing a beam of 5–10 keV electrons onto the appropriate target. By reflecting the X rays off a grazing-incidence mirror, the contaminating bremsstrahlung radiation is reduced to 2%. The focused X rays are then aimed at selected subcellular targets using rapid automated cell-finding and alignment procedures; up to 3000 cells per hour can be irradiated individually using this arrangement. © 2001 by Radiation Research Society

INTRODUCTION

There is now considerable interest in the application of microirradiation techniques for radiobiological applications. The strength of the microirradiation technique lies in its ability to deliver precise doses of radiation to selected individual cells *in vitro* or to preselected targets within cells. This paper reports on the development and characterization of a novel focused ultrasoft X-ray microprobe for irradiating subcellular targets individually with submicrometer accuracy. Worldwide, only two other microbeam facilities are in routine use for radiobiology: a charged-particle microbeam at the Gray Laboratory, developed and operated by ourselves (*1, 2*), and the Radiological Research Accelerator Facility at Columbia University, New York (*3*), also using

charged particles to microirradiate cells. Several other facilities are planned or are at various stages of development (*4*). The X-ray microprobe makes use of 278 eV carbon K-shell X rays (and recently 1.49 keV aluminum K-shell X rays) and has been developed alongside our existing charged-particle microbeam to address problems specific to low-LET radiations (insofar as electrons induced by ultrasoft X rays resemble the track ends of low-LET electrons), to study the low-dose region of the dose–response curve, and to address problems where very precise targeting accuracy and dose delivery are required (*5*). Techniques for focusing ultrasoft X rays to produce very fine probes are now well established (*6*). Unlike charged particles, ultrasoft X rays interact almost entirely by the photoelectric effect and are therefore subject to very little scatter. To date, the finest probes have been obtained in the field of X-ray microscopy by using circular diffraction gratings known as "zone plates". The development of zone plates has advanced significantly in recent years, and it is now possible to make devices that can focus X rays to diameters of 50 nm or less at energies of a few hundred electron volts. By comparison, the most accurate collimated charged-particle microbeams have an aiming accuracy of about 2–5 μm (*2*). It is not expected that the accuracy can be improved significantly for light ions, even if focusing or finer collimators are used, because of the effects of scattering.

The emphasis of this paper is on the development and characterization of the facility. Subsequent papers will report the findings from a number of biological studies currently under way. The development of microirradiation approaches has coincided with important new findings regarding mechanisms of the action of radiation in cells and tissues. A major interest is in the role of nontargeted effects, where *direct* damage to cellular DNA does not appear to be a requirement. For example, Nagasawa and Little (*7*) observed sister chromatid exchanges in 30% of cells after exposure to α particles such that only 1% of cell nuclei are actually hit. A similar finding has been reported by Deshpande *et al.* (*8*) in primary human fibroblasts, while Hickman *et al.* (*9*) found greater than expected levels of TP53 in α-particle-irradiated epithelial cells. Zhou *et al.* (*10*) used

the Columbia University microbeam to investigate the mutagenic effect of α particles in mammalian cells. They found a higher mutant yield than expected when 5–10% of the cells were irradiated with 20 α particles each, indicating a bystander effect. Our own work (11, 12) using the Gray Laboratory charged-particle microbeam provided direct evidence for a bystander effect between irradiated and non-irradiated cells. It is also believed that inter- and intracellular signaling may be implicated in the phenomenon of genomic instability, where alterations to the genome of surviving cells lead to delayed effects such as apoptosis, mutations and chromosomal instability (13), and that this may be highly dependent on LET in some systems (14). Other studies have provided direct evidence that cytoplasmic targets are important in the production of, for example, radiation-induced mutations (15). Here the charged-particle microbeam and the X-ray microprobe will have complementary roles in studying the LET dependence of nontargeted effects. The exquisite resolution afforded by focused ultrasoft X rays will allow important questions regarding the locations and mechanisms of subcellular targets to be addressed carefully. Note that another possibility for developing a low-LET microbeam exists, and that is to use a fine beam of electrons. Indeed, such facilities are being developed, and a recent related microdosimetric study showed that the energy deposited by a 25 keV electron track is likely to be contained within a typical mammalian HeLa cell, but that the energy will be dispersed nonuniformly through the cell (16).

Radiobiology Using Ultrasoft X Rays

Ultrasoft X rays are loosely defined as having energies from a few hundred eV to a few keV. The radiobiological properties of ultrasoft X rays have been studied and reported previously. Studies of clonogenic survival (17–19), mutation (17), DNA damage (18), and chromosome exchanges (20) show that ultrasoft X rays are significantly more effective than conventional penetrating X rays and that their effectiveness increases with decreasing X-ray energy. The shapes of the curves fitted to the data for ultrasoft and conventional X rays are statistically indistinguishable from one another, implying that the enhanced effectiveness is purely dose-modifying. These observations, and the very short ranges of the secondary electrons that arise from photoelectric absorption (~5 nm for carbon K-shell X rays, ~70 nm for aluminum K-shell X rays), support the view that it is very local energy depositions, on the nanometer scale, that are principally responsible for the observed radiobiological effects. Consequently, we can consider a beam of focused ultrasoft X rays to be a model of the biologically effective part of a conventional low-LET electron track. As an energetic electron passes through the cell, it will produce clusters of ionizations similar to those produced by individual ultrasoft X rays. Other studies using ultrasoft X rays are more controversial. A series of related

studies (21–23) following on from the work of Raju et al. (19) showed that the effectiveness of ultrasoft X rays increases with increasing cell thickness, casting doubt on the concept of "mean dose" at the cellular level. The targeting capability of the X-ray microprobe could be used to investigate this unexpected finding further.

METHODS

To use zone-plate focusing optics, monochromatic radiation is required. Such radiation is readily available from synchrotron sources, and is the source of choice with regard to energy selection and brightness. However, it is also possible to develop "benchtop" monochromatic sources based either on laser plasma-generated X rays or on the production of characteristic X rays by electron (or charged-particle) bombardment of a target. Using electron bombardment is clearly advantageous from the point of view of cost and convenience.

The impetus in X-ray microscopy has been to develop zone plates that operate in the so-called water window (i.e. between the K-shell absorption edges of oxygen and carbon) where good image contrast is observed in tissue-like materials. For this reason, we initially chose to base the microprobe on 278 eV carbon K-shell X rays, generated by electron bombardment of a carbon (graphite) target. A drawback of using carbon K-shell X rays is their relatively poor penetration in tissues (the 1/e attenuation length is only 1.9 μm) and is one reason why we have also recently developed the facility to use 1.49 keV aluminum K-shell X rays (1/e attenuation length, 7.2 μm). However, the zone plates for focusing aluminum K-shell X rays have only recently become available to us and will not be discussed in this paper.

The development of the X-ray microprobe cell irradiation facility can be divided into three key areas: the source of radiation, the X-ray focusing assembly, and the arrangement for finding and aligning targets with the X-ray focus. Another important area of development is the design and implementation of the biological assays of radiation damage for use with this facility. Some assays, such as those measuring micronucleus formation and apoptosis, have been reported previously (11, 12) in connection with our charged-particle microbeam. The use of other assays will be described in subsequent publications.

The Microfocus X-Ray Source

The microfocus source is used to generate a micrometer-sized source of X rays suitable for imaging by the focusing assembly. Characteristic X rays of carbon (278 eV) or aluminum (1.49 keV) are generated by focused electron bombardment of a thick carbon or aluminum target. The source was originally built by the National Physical Laboratory, UK (NPL) to operate as part of an X-ray microscope and was donated to the current project when the NPL developed a second facility. The mechanical construction of the source is mostly unchanged; however, the internal electrical wiring, the high-voltage power supplies, and the control electronics have been replaced.

Figure 1 depicts the X-ray microfocus source. The source of electrons is a heated "hairpin" tungsten filament normally used for electron microscope applications (Agar Scientific, UK); it forms part of an electron gun assembly mounted horizontally within a 285 × 175 × 110-mm (length × width × height) machined aluminum block. All internal cavities within the aluminum block are maintained at ~10^{-5} mbar using a small turbo-molecular pump ("backed" by a rotary pump) mounted to a port on one side of the block. The X-ray source and other apparatus that make up the irradiation facility are supported on a vibration-isolated optical table. Mass damping of the backing-line vacuum hose is used to prevent vibrations from the rotary pump reaching the source.

The electron gun can be operated at voltages up to −30 kV relative to the carbon target. The filament is mounted just behind the hole in a brass Wehnalt grid. The grid is normally maintained at a low (~500 V)
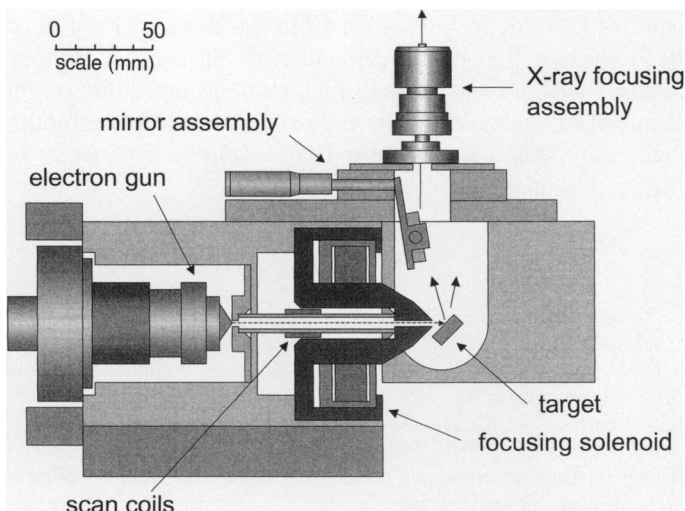
FIG. 1. The X-ray microfocus source. Electron bombardment is used to generate a micrometer-sized source of characteristic X rays. A mirror between the X-ray source and the focusing assembly removes unwanted bremsstrahlung radiation.

FIG. 2. The arrangement of the zone plate and masks (not to scale) used for selecting first-order diffracted X rays. Properly aligned, the masks pass first-order diffracted X rays (a), but block other diffracted orders (b).

positive voltage relative to the filament; by adjusting this voltage, it is possible to regulate the current passing through the grid. The grid also serves to suppress electrons not generated at the tip of the filament. Electrons emerging from the grid aperture pass horizontally down an 80-mm × 9-mm-diameter flight tube within a water-cooled, electromagnetic solenoid lens, with a focal length of 3 mm. The diameter of the electron beam at the focus is about 2–5 μm. The electrons strike a thick target mounted at 45° to the horizontal axis of the incident electrons and at 45° to the vertical axis of the X-ray focusing assembly. The target assembly is isolated electrically from the rest of the source, so that the current due to the incident accelerated electrons can be monitored. As an aid to focusing the electrons onto the target, two sets of scan coils are mounted around the electron flight tube. These can be used to scan the electron beam across part of the target; by displaying the current generated in the target using an oscilloscope (with the time base synchronized to the scan period), it is possible to see "structure" in the oscilloscope trace, but only when the electrons are sharply focused onto the target. Once a focused condition is achieved, the scanning action is disabled, although a d.c. current is sometimes applied to the scan coils to optimize the X-ray output.

In addition to characteristic radiation, the electron bombardment of the target will produce a continuum of bremsstrahlung with a maximum energy equivalent to the energy of the incident electrons. This radiation is undesirable because it will not be focused correctly by the zone plate, and can be significantly more penetrating than the characteristic X rays. The bremsstrahlung component is removed by reflecting the radiation off a 25-mm-diameter silica mirror mounted between the carbon target and the focusing assembly (see Fig. 1). At shallow angles of incidence, the mirror will reflect most of the carbon K-shell X rays and will absorb photons of higher energy. The mirror is mounted on an adjustable stage that also supports the X-ray focusing assembly. Two micrometers are used to translate the stage and tilt the mirror independently. The mirror is rotated to optimize the incident angle (typically, about 2°), while translation of the stage maintains the correct geometry of the source, mirror and focusing assembly as the mirror is rotated.
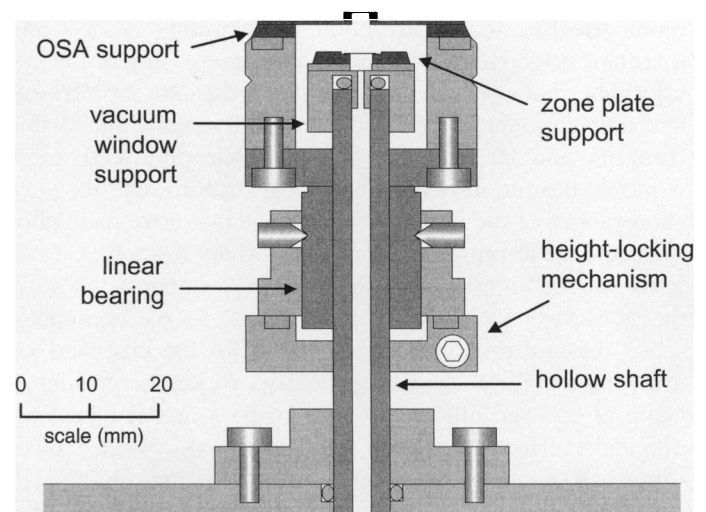
The X-Ray Focusing Assembly

The production of fine X-ray probes can now be achieved by the use of X-ray optics developed for high-resolution X-ray microscopic imaging. The finest X-ray probes have been obtained using zone plates. These are circular diffraction gratings with radially increasing line densities, such
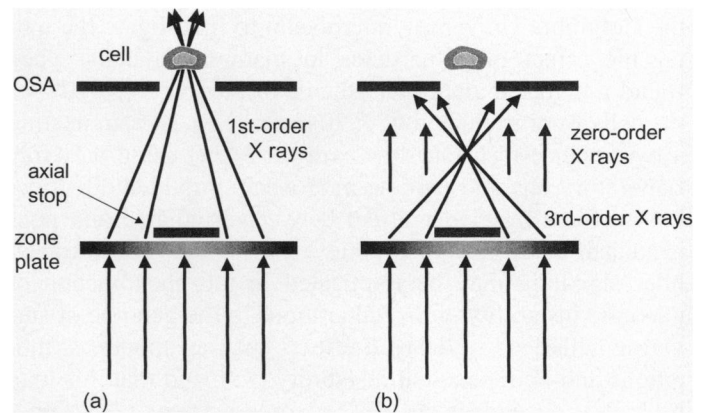
that diffracted X rays are brought to an axial focus (*6, 24*). Using facilities available at King's College, London, we have designed and manufactured zone plates specifically for use with this project. The zone plates are made from tungsten that is deposited on a 100-nm-thick silicon nitride substrate by electron beam lithography. Most recently, we have acquired zone plates for focusing carbon K-shell and aluminum K-shell X rays, manufactured at the Paul Scherrer Institute (Villigen, Switzerland). Our current carbon K-shell zone plates have a radius of 200 μm and a focal length of ~9 mm for first-order diffracted X rays. The first-order efficiency of these zone plates is typically 7–14%.

As with other diffraction devices, several diffracted orders are produced, and the unwanted orders must be prevented from reaching the cells, because they will not be appropriately focused. To do this, an arrangement of masks is used that allows only the first-order diffracted X rays to reach the target. The principle is illustrated in Fig. 2. The masks consist of a 100-μm-diameter axial stop mounted directly onto the zone plate (this is added during the manufacture of the zone plate) and a 12.5-μm-diameter axial pinhole (the order selecting aperture, or OSA) close to the first-order focus. A compact assembly for supporting the zone plate and for micro-aligning and supporting the OSA has been developed. The assembly, which is illustrated in Fig. 3, and has been designed to fit comfortably within the 50-mm aperture of a micropositioning stage used


FIG. 3. The focusing assembly used to align the vacuum window, zone plate and masks.
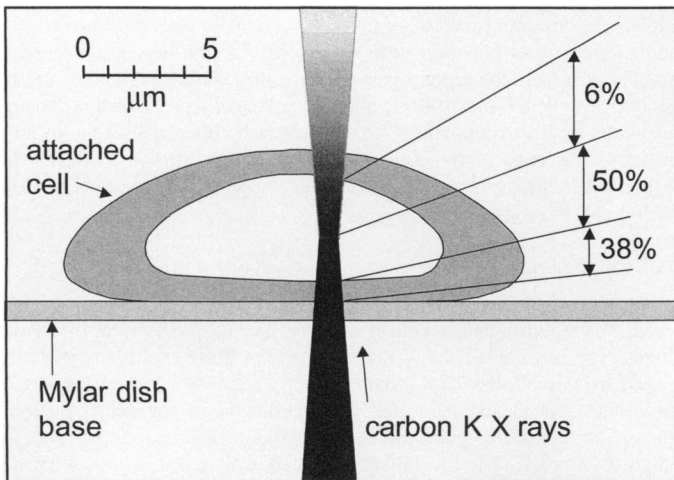
FIG. 4. Deposition of the focused carbon K-shell X rays in an attached V79 mammalian cell. The figures indicate the percentages of the beam incident on the lower cell surface that are absorbed in the various parts of the cell.

to support the cell dish. The assembly allows horizontal (two-axis) alignment of the zone plate with respect to the vacuum window and three-axis alignment of the OSA. The assembly is based on a 60-mm-long × 8-mm-diameter hollow shaft that supports a nonrotating precision linear bearing. A 0.5 × 0.5-mm silicon nitride vacuum window (100 nm thick) is mounted at the end of the shaft using a cap that forms a vacuum seal. The zone plate is bonded to a 13-mm-diameter steel disc that is magnetically coupled to this cap, such that it can be maneuvered easily to the correct position (i.e. directly above the window). The OSA is supported by the linear bearing such that it is free to move vertically relative to the zone plate. It is also magnetically coupled to its support to facilitate alignment in the horizontal plane. The height-locking mechanism is decoupled from the linear bearing by magnets to prevent a lateral movement of the OSA when the locking bolt is tightened. To minimize attenuation of the X rays, the enclosed space between the vacuum window and the OSA is flushed continuously with helium gas and is partly vented through the OSA to flush the small gap between the OSA and the cell dish. The alignment of the focusing assembly is discussed in the Results section.
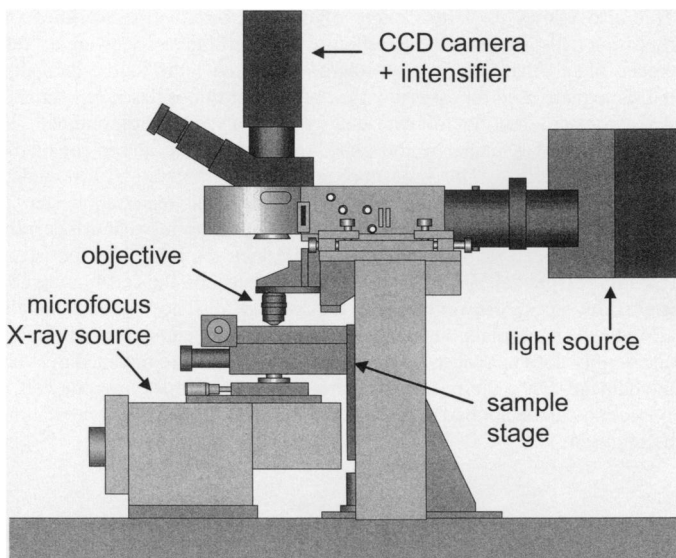
FIG. 5. The imaging and alignment system used to find and position cells at the X-ray focus.

Dosimetry

The X-ray output is characterized using a custom-built proportional counter that operates in a photon counting mode. This detector is designed to screw into the microscope objective mount that is part of the in situ cell imaging arrangement (see the next section) and has a 9-mm-long × 6-mm-diameter sensitive volume, with a 0.9-μm-thick Mylar window located at the focus of the zone plate. The attenuation of the X rays through the proportional counter window is the same as that through the base of the dish to which the cells are attached. During operation, the counter is flushed with P10 gas (10% methane, 90% argon) at atmospheric pressure. The anode is polarized to 1900 V, and conventional nucleonics are used to amplify and shape the signal, which is then displayed as a pulse-height spectrum on a multichannel analyzer. The proportional counter is used routinely for all setting up and X-ray optical alignment procedures. It is also used to measure the dose rate from the source, expressed initially as the number of focused carbon K-shell photons per second incident on the cell surface. However, the low-energy part of the broad peak representing carbon K-shell photons cannot be discriminated from the noise pulses; therefore, counts only in the higher-energy half of the peak are counted (and the counts are doubled). Choosing a method to express the cell dose when targeted and partially penetrating radiations are used can be problematic. The dose to each cell is nonhomogenous and is dependent on the cell morphology. This is illustrated in Fig. 4, which shows the dose distribution in a Chinese hamster V79 cell exposed to a focused beam of carbon K-shell X rays. In this example, about 40% of the dose is deposited in the first micrometer of the cell (i.e. in the cytoplasm), about 50% in the lower half of the nucleus and a further 6% in the upper half of the nucleus. A V79 cell would need to absorb about 10,000 carbon K-shell X-ray photons to produce an average a dose of 1 Gy in the nucleus (based on the absorbed energy in the nucleus divided by the nuclear mass). Greater dose uniformity along the beam axis can be achieved by using more penetrating photons, such as aluminum K-shell X rays.

Cell Imaging and Alignment

The support, imaging and accurate alignment of cells at the X-ray focus are critical to the overall precision of the X-ray microprobe. Currently, cells to be irradiated are attached to a 0.9-μm-thick Mylar membrane (Goodfellow Ltd., UK) that forms the base of a cell dish. The design of the cell dish is described by Folkard et al. (1). The dishes are clamped to a two-axis, stepper-motorized microscope stage (Märzhäuser, Germany) with a resolution of 250 nm, a reproducibility of ±1 μm, and an absolute accuracy of ±3 μm. The stage is supported on a vertically mounted linear bearing, and it can be micropositioned in the vertical direction using a d.c. motor coupled to a precision lead screw. A "linearly variable differential transformer" (LVDT) position sensor is used to provide closed-loop feedback control of the stage height.

The imaging and alignment system is depicted in Fig. 5. It based on the original arrangement developed for our charged-particle microbeam facility (1), but with a number of improvements. In fact, the microbeam system has subsequently been refurbished such that where possible, the two systems match each other. In the present system, cells are viewed in situ using an infinity-optics microscope assembled using components from the Olympus BX range (Olympus, UK). Specifically, a light condenser, lamp housing (fitted with a 100-W mercury lamp), and four-cube filter turret are used to provide epifluorescence illumination of the cells. An objective lens is supported on a custom-built mount that can be moved precisely up to 2 cm in the vertical direction by a calibrated stepper-motor-driven micrometer. The objective mount and the Märzhäuser stage are controlled by a three-axis stage driver (Mac4000, Märzhäuser, Germany). In this arrangement, cell focusing is achieved by raising and lowering the objective lens rather than the sample stage (made possible by the use of infinity-corrected optics). This is necessary because the height of the sample is fixed by the position of the zone-plate focus (in this respect, it differs from the microbeam system, which does not use a

position-adjustable objective). As described below, the micropositioning capability of the objective lens is critical to aligning the X-ray focusing assembly and to locating cells at the X-ray focus.

The cells are stained with a UV-fluorescent dye. The type of dye used will determine which subcellular features are observed. For example, the DNA-binding dye Hoechst 33258 is frequently used to highlight the cell nucleus. As with our charged-particle microbeam, it is important to minimize the dye concentration, and the UV-radiation dose. The cells can be viewed either using a standard trinocular eyepiece or, more typically, with an intensified, charge-coupled device (CCD) camera. Our camera has been developed in-house and uses a Gen2 image intensifier, coupled through a fiber-optic taper to a video-rate CCD imager (Philips XX1666/CJ10, coupled to a Philips FTM800 chip). Our unit gives independent programmable control of black level, CCD gain, and image intensifier gain. Typical sensitivities of less than 1×10^{-5} lux are obtained, with around 25 line pairs per millimeter resolution at the photocathode faceplate. The CCD output is a standard interlaced video signal which is digitized using a Matrox "Pulsar" frame grabber to 8-bit resolution. A modification to the CCD timing logic allows it to be operated at full framing rates (25 per second) as well as in an integrating mode where the intensifier output may be collected over periods of 255 40-ms frames (i.e. around 10 s), at which point CCD dark current becomes excessive. To reduce the UV-radiation dose to the cells, a leaf-shutter has been installed in the UV-excitation light path and has been synchronized to open only during image acquisition. Typically, a static image of the cells is acquired as a "snapshot" within the 100-ms opening time of the leaf-shutter. We are currently developing an off-line imaging system for finding cells that does not involve the use of cell dyes or UV illumination.

All key operations of the microprobe are controlled using a Pentium PC, including movement of the three-axis stage driver (via an RS232 interface), display of microfocus source status, the acquisition of the CCD camera image, and display and image processing. A software user interface has been developed that is based on an image analysis software package (Visilog, France) running under Windows NT. The same software is implemented on both the microprobe and the microbeam facilities, so that software developments are of immediate benefit to both systems (clearly, however, some features of the software are facility-specific). A graphical user interface (GUI) has been developed for routine operation of the software. The user is presented with a range of pull-down menus and virtual control panels for inputting and displaying information. One key set of panels allows the user to select from a range of strategies for irradiating cells. As new experiments are devised, appropriate panels to control the irradiations are implemented. One type of experiment often performed is to irradiate all cell nuclei in a region of the dish with the same dose. There may be a few hundred cells within a predefined 4.5-mm² region. To locate these cells, an automated procedure views the region as a series of 80 slightly overlapping frames, where each frame is the field of view of the microscope (0.45 mm by 0.7 mm, using a 20× objective). The computer images and then analyzes each frame in turn and uses a boundary-following algorithm to establish the optical center of gravity of each fluorescent object (i.e. each cell nucleus). The coordinates of each object are logged, along with a number of other parameters (size, intensity, etc.) used to distinguish the cells from other fluorescent objects. It takes about 2 s to acquire and analyze each frame; all the cells in the region can therefore be identified in about 3 min.

For reliable positioning accuracy, the optical aberrations in the image must be considered; otherwise, the coordinates assigned to a cell may not be correct (particularly for cells imaged at the edge of the viewing area, where the aberrations are greatest). To overcome this problem, a distortion "look-up table" is created by imaging a small, bright object (an LED behind a 3.5-μm-diameter pinhole) as it moves in a fine grid pattern covering the image area. By image-analyzing the grid pattern, the computer can then calculate the optical distortions and make appropriate corrections to the assigned coordinates of objects in all subsequent images. If better positioning accuracy is required, a "two-pass" system is used, in which each cell is moved to the nominal irradiation position and re-imaged, and then moved a second time if any residual error is discovered.

However, this procedure does give the cell a second exposure to UV radiation, so it is not used unless required. For the best possible positioning accuracy, the second pass is performed with a higher-power objective installed (40×–100×), and for each cell, the target is located manually by the experimenter. This is achieved either by using a joystick to move the stage or by using "point-and-click" method in which the experimenter uses an on-screen computer mouse pointer to select the part of the cell to be irradiated.

Cell Irradiation Procedure

Once all the cell coordinates are logged, the irradiation step may proceed. To microirradiate a cell, it must be located precisely at the X-ray focus. The location of the X-ray focus in the horizontal plane is established by viewing the OSA (when correctly aligned, the X-ray focus will be at the center) and recording the coordinates of the center position (using an on-screen point-and-click method). The cell must also be aligned vertically. The focal plane of the zone plate is at a known (small) distance above the OSA, so by raising the microscope objective by this amount (having previously focused on the OSA), any cell moved to the correct position in the horizontal plane will also be at the correct height, provided that it is in focus when viewed through the objective. Once this condition is established, the automated irradiation sequence may be initiated. With the source energized, each cell is moved, in turn, to the irradiation position and exposed to a preset dose of X rays, by giving a timed exposure. This method is reliable provided that the microfocus source target current (which is monitored) is stable. At present, a shutter is not used to start and stop each cell exposure. Instead, the exposure is terminated by rapidly moving to the next cell once the desired dose has been reached. A typical cell exposure may take just a second or two, so that region of the dish with, say, 500 cells will be irradiated in about 10–20 min. Other types of experiments, such as those connected with the bystander effect, may require only a few cells or even just a single cell to be irradiated (*11*).

After all the cells have been exposed, the dishes are transferred to an incubator, or they receive some other appropriate postirradiation treatment prior to scoring. Some assays, such as the clonogenic assay, make use of the microprobe's revisiting capability to assess damage through the microscope on a cell-by-cell basis. This is typically done 3 days after the irradiation. To revisit cells, the dish is returned to the stage and the original set of coordinates are recalled and used to move each cell in turn to the center of the field of view. To do this reliably, a registration step is required to establish the stage coordinate system relative to the CCD camera (which may change day to day due to routine maintenance, etc.). This also allows us to use either of our microirradiation facilities for revisiting cells. Registration is achieved by installing and viewing a "reference plate" that comprises a micrometer-sized light source (actually, the same plate used for assessing the optical distortions described earlier). An automated routine follows and image-analyzes a programmed sequence of moves made by the plate, from which the alignment of the stage is ascertained. This procedure takes just a minute, and it is undertaken at the beginning of each day. Although the registration step is accurate, there is a 10–20-μm uncertainty in positioning that arises from removing the cell dish from the stage and then returning it to the stage (for this reason, cell dishes are not removed between the cell-finding and irradiation steps). However, since the average distance between neighboring cells is normally at least hundreds of micrometers, this positioning uncertainty does not cause any ambiguity when cells are revisited to assay the damage. Once the positioning error is established for any one cell, a correction can be applied to the remaining cells should accurate revisiting be required.

RESULTS

X-Ray Output

The number of characteristic X rays generated at the target of the microfocus source will be proportional to the
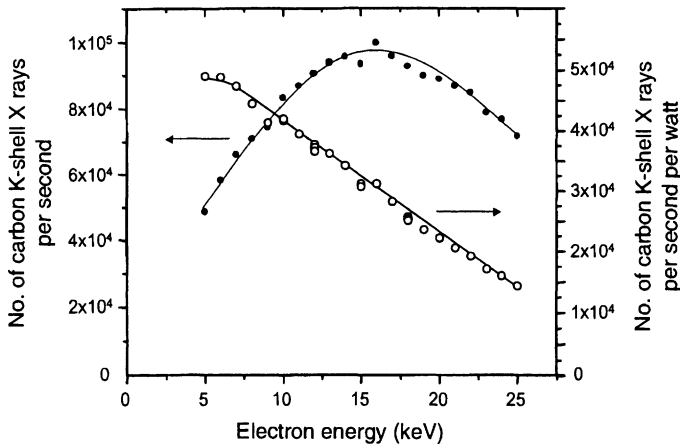
FIG. 6. The output of X rays through the vacuum window as a function of electron accelerating voltage for a 200-μA electron beam, expressed either per second (closed symbols) or per second per watt (open symbols).

incident electron current and will be a function of the accelerating voltage (but not through simple proportionality). To achieve the best possible cell throughput, it is necessary to maximize the X-ray output. The proportional counter has been used to establish the optimum operating conditions. Figure 6 shows the output of carbon K-shell X rays as a function of the accelerating voltage, at constant current, through a 0.5-mm² silicon nitride window (with no zone plate present). The X-ray output increases with voltage up to 15 kV and then decreases. The reduction beyond 15 kV occurs because the electrons are penetrating deeper into the target, and increasing fractions of the X rays are being attenuated within the target. If the same data are expressed as the output of carbon K-shell X rays per watt, it can be seen that the source is more efficient at lower voltages. For this reason, the original high-voltage, low-current (up to 30 kV, 1 mA) accelerating power supply was replaced with a 10 kV, 10 mA unit (Applied Kilovolts, UK) so that higher currents could be achieved. There is also a considerable advantage in operating at 10 kV or less, because the likelihood of electrical breakdown is greatly reduced, and less bremsstrahlung is produced. In practice, beam currents much beyond 3 mA (measured at the filament) shorten the lifetime of the filament; therefore, the source is usually operated at 9–10 kV, 3 mA (or about 550 μA, measured at the target) for near-maximum output. No special measures are required to cool the target under these operating conditions. However, cooling may be required when an aluminum target (which has a lower melting point) is eventually used at high powers. When the microfocus source is operating under optimum conditions, the output of carbon K-shell X rays through the exit widow of the source is about 5 × 10⁵ photons s⁻¹. This will yield about 1.3 × 10⁴ photons s⁻¹ in the first-order focus of our most efficient zone plate, which produces a dose rate of about 1 Gy s⁻¹ when a V79 cell (or a cell of similar size) is irradiated. The losses that occur within the focusing assembly are summarized in Table 1.

TABLE 1
Carbon K-Shell X-Ray Losses that Occur in Various Parts of the X-Ray Focusing Assembly at Optimum Operating Conditions

Position	Percentage reduction	Number of carbon K-shell X rays per second
Output through 0.5 × 05-mm Si_3N_4 window		4.8 × 10⁵
Incident on 200-μm-radius zone	50.3%	2.4 × 10⁵
After transmission through 60 nm Si_3N_4 zone plate substrate	61.5%	1.5 × 10⁵
After transmission through 9 mm helium	62.0%	9.3 × 10⁵
In zone plate first-order focus	14.5%	1.3 × 10⁵

*Notes.* Values given are for a 550-μA target current at 9 kV. The output through the window and the number of X rays in the first-order focus are measured data; the remaining values are calculated.

X-Ray Spectrum

The proportional counter has been used to investigate the energy spectrum of the X rays generated by the microfocus source and therefore to estimate the fractions of characteristic and bremsstrahlung being produced. The bremsstrahlung component is removed by a mirror mounted between the carbon target and the focusing assembly. Figure 7 shows the measured energy spectra as a function of the incident angle of the radiation to the mirror. It is evident that as the angle of the mirror is increased, the relative fraction of bremsstrahlung is substantially reduced. Beyond about 3°, only a single broad peak (the broadness corresponding to the response function of the counter) centered on the carbon K-shell X-ray peak is observed. A further increase in the incident angle will reduce the carbon K-shell X-ray output. The source is normally operated with a mirror incident angle of 2–3°. Using this geometry, it has been estimated that 5% of X rays exiting the vacuum win-
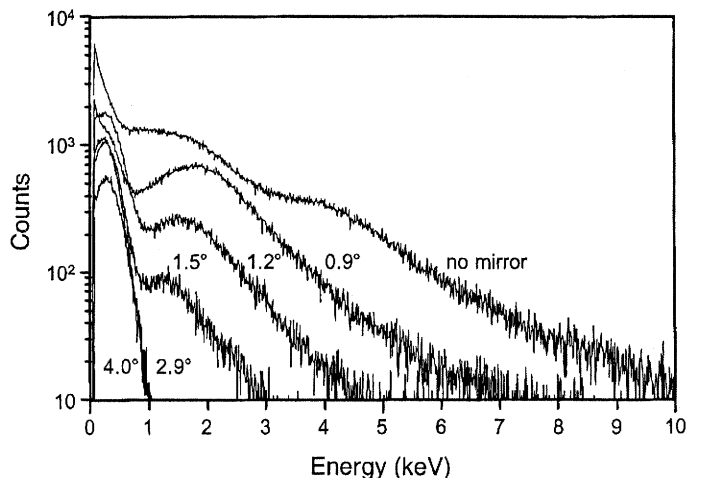
FIG. 7. The photon energy spectrum as a function of the incident angle of the mirror for X rays produced by a 15 kV electron beam.
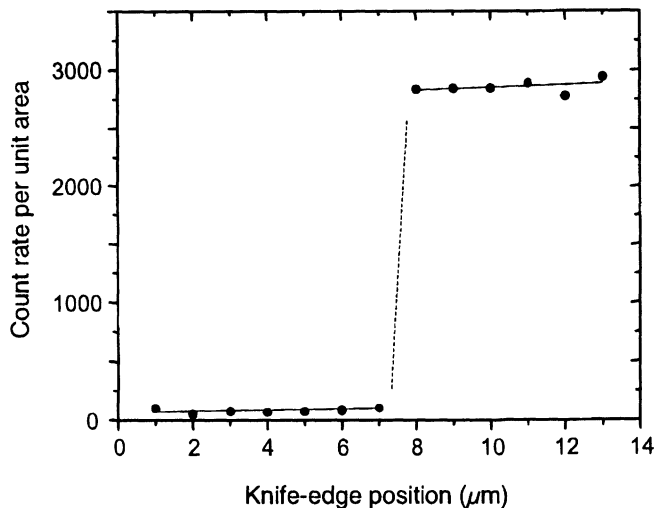
FIG. 8. The output of X rays per unit area exposed as a knife-edge (made from 3-μm-thick Mylar) is scanned through the focus above a 12.5-μm-diameter OSA.

dow are due to bremsstrahlung. After focusing by the zone plate, only 2% bremsstrahlung remains.

Focusing

The alignment of the focusing assembly is a two-step process. First, the zone plate must be aligned above the exit window of the microfocus source. This is achieved by nudging the magnetically coupled zone plate to the correct position while viewing with the microscope (the correct position having been established by observing the position of the window without the zone plate present). Second, the OSA must be aligned above the zone plate. The procedure for this is not so simple, as precise alignment is required in all three planes. Setting the correct height is achieved by first focusing on the zone plate, then raising the objective by exactly the zone plate focal distance, and then adjusting the height of the OSA support, such that the OSA is in the same plane as the optical focus. The OSA is aligned laterally, using the micropositioning stage that normally supports the cell dish. By clamping the OSA to the stage, it is possible to move the OSA (which is magnetically coupled to its support) precisely in the horizontal plane. The exact position is then found by carefully moving the OSA while monitoring the fluence of X rays through the OSA using a proportional counter. Maximum fluence is achieved when the OSA is aligned with the X-ray focus.

The position of the X-ray focus is checked by scanning a "knife edge" through the beam at the X-ray focal plane (just above the OSA, if correctly aligned). This is illustrated in Fig. 8, which shows the number of X rays reaching the proportional counter as the edge of a 3-μm-thick Mylar film is moved through the focus. It is evident that the Mylar intercepts the entire beam within a 1-μm change of position. If the Mylar were not in the focal plane, a more gradual interception of the beam would be observed. Note that

the calculated depth of focus of the X-ray beam is about ±6 μm (for a 10% increase in beam diameter).

Cell Alignment and Cell Throughput

The targeting capability of the microprobe cannot be fully exploited unless cells can be positioned with a comparable accuracy. Nevertheless, the majority of experiments simply require that the cell nucleus be targeted, for which an accuracy of a few micrometers is sufficient. As discussed in the Methods section, three methods for finding and locating cells have been established. While high accuracy might seem desirable, the most accurate methods currently give the highest UV-radiation exposure to the cells and are the least favorable in terms of cell throughput.

The positioning accuracy of the most precise method (in which the subcellular target is selected cell by cell using a mouse pointer) is limited by the image quality and the resolution. This is somewhat variable, since it depends on staining conditions, cell morphology, etc., but with a good-quality image, this method can achieve submicrometer positioning. Clearly, the throughput of cells is determined largely by the speed at which the experimenter can identify and register the chosen targets, although this generally takes just a few seconds per cell. The next most precise positioning method (the "two-pass" method) is a variation of a technique used with our charged-particle microbeam for several years. The accuracy of this approach has been investigated and reported previously (*25*). In this study, it was concluded that >98% of cells are positioned within 1.5 μm, >81% are within 0.75 μm, and >62% are within 0.5 μm. The final positioning method (using one pass of the imager) has been implemented recently on both our microirradiation facilities to achieve a fast throughput of cells. Using this method with the particle microbeam, it is now possible to find and irradiate up to about 7000 cells per hour (15 min for cell finding, then 45 min for exposure). The same cell throughput could be achieved on the microprobe for finding cells; however, at present, the irradiation step is slower, depending on the X-ray dose rate and the desired dose to each cell. If it takes about 1 s to irradiate each cell, then the cell throughput (for finding, then irradiating) is typically about 3000 cells per hour. Faster cell throughputs are expected as improvements to the source efficiency are implemented.

The positioning accuracy of the one-pass method has been investigated by imaging a 3.5-μm-diameter back-illuminated pinhole at various locations within the field of view, then allowing the computer to move the pinhole to the irradiation position after correcting for optical distortions using the stored look-up table. The pinhole is then reimaged, and the error in its position is determined. By doing this systematically across the entire screen, it is possible to generate a map of the positioning error as a function of the screen position where the object is found. As expected, in this mode, the position accuracy is dominated by the absolute accuracy of the stage. About 43% of cells are

positioned with an accuracy <1.5 μm, 78% are positioned <2.5 μm, and all cells are positioned <3.75 μm. This is the least precise of the three targeting methods, but it is still just accurate enough for reliable nuclear targeting of most cell types. Nevertheless, we wish to improve the accuracy of this mode of operation and are currently developing a faster and more accurate stage (using closed-loop position feedback) for use with both of our microirradiation facilities. We envisage achieving significant improvements in accuracy and speed using the one-pass alignment method once this stage is fitted.

CONCLUSIONS

In this report, we have described the development and characterization of a unique facility that uses focused ultrasoft X rays as the basis for submicrometer single-cell irradiation. There are a number of benefits to using this approach, most notably the fact that it generates a very fine probe that is not degraded by scattering. It should also be evident that the development of such a facility is within the reach of many more laboratories than is a microbeam based on accelerated charged particles. Like many technologically based projects, improvements are always being sought and implemented. As such, this report should be viewed as a "snapshot" of the facility at a particular stage of its development. Future developments, such as off-line cell finding that does not require UV radiation and an improved micropositioning stage, are under way and will be implemented in the future.

ACKNOWLEDGMENTS

REFERENCES

1. M. Folkard, B. Vojnovic, K. M. Prise, A. G. Bowey, R. J. Locke, G. Schettino and B. D. Michael, A charged-particle microbeam: I. Development of an experimental system for targeting cells individually with counted particles. *Int. J. Radiat. Biol.* **72**, 375–385 (1997).

2. M. Folkard, B. Vojnovic, K. J. Hollis, A. G. Bowey, S. J. Watts, G. Schettino, K. M. Prise and B. D. Michael, A charged-particle microbeam: II. A single-particle micro-collimation and detection system. *Int. J. Radiat. Biol.* **72**, 387–395 (1997).

3. C. Geard, D. J. Brenner, G. Randers-Pehrson and S. A. Marino, Single-particle irradiation of mammalian cells at the Radiological Re-search Accelerator Facility: Induction of chromosomal changes. *Nucl. Instrum. Methods* **B54**, 411–416 (1991).

4. M. Folkard, K. M. Prise, B. Vojnovic, S. Gilchrist, G. Schettino, O. V. Belyakov, A. Ozols and B. D. Michael, The impact of microbeams in radiation biology. *Nucl. Instrum. Methods*, in press.

5. G. Schettino, M. Folkard, K. M. Prise, B. Vojnovic, T. English, A. G. Michette, S. J. Pfauntsch, M. Forsberg and B. D. Michael, The soft X-ray microprobe: A fine sub-cellular probe for investigating the spatial aspects of the interaction of ionizing radiation with tissue. In *Microdosimetry. An Interdisciplinary Approach* (D. T. Goodhead, P. O'Neill and H. G. Menzel, Eds.), pp. 347–350. Royal Society of Chemistry, Cambridge, 1997.

6. C. A. MacDonald and W. M. Gibson, X-ray and neutron optics. In *Handbook of Optics Vol. III. Classical, Vision and X-Ray Optics* (M. Bass, J. M. Enoch, E. W. van Stryland and W. L. Wolfe, Eds.), pp. 19.1–30.17. McGraw-Hill, New York, 2001.

7. H. Nagasawa and J. B. Little, Induction of sister chromatid exchanges by extremely low doses of α-particles. *Cancer Res.* **52**, 6394–6396 (1992).

8. A. Deshpande, E. H. Goodwin, S. M. Bailey, B. L. Marrone and B. E. Lehnert, Alpha-particle-induced sister chromatid exchange in normal human lung fibroblasts: Evidence for an extranuclear target. *Radiat. Res.* **145**, 260–267 (1996).

9. W. Hickman, R. J. Jaramillo, J. F. Lechner and N. F. Johnson, α-particle-induced p53 expression in a rat lung epithelial cell strain. *Cancer Res.* **54**, 5797–5800 (1994).

10. H. Zhou, G. Randers-Pehrson, C. A. Waldren, D. Vannais, E. J. Hall and T. K. Hei, Induction of a bystander mutagenic effect of alpha particles in mammalian cells. *Proc. Natl. Acad. Sci. USA* **97**, 2099–2104 (2000).

11. O. V. Belyakov, A. M. Malcolmson, M. Folkard, K. M. Prise and B. D. Michael, Direct evidence for a radiation-induced bystander effect of ionising radiation in primary human fibroblasts. *Br. J. Cancer* **84**, 674–679 (2001).

12. K. M. Prise, O. V. Belyakov, M. Folkard and B. D. Michael, Studies of bystander effects in human fibroblasts using a charged particle microbeam. *Int. J. Radiat. Biol.* **74**, 793–798 (1998).

13. S. A. Lorimore, M. A. Kadhim, D. A. Pocock, D. Papworth, D. L. Stevens, D. T. Goodhead and E. G. Wright, Chromosomal instability in the descendants of unirradiated surviving cells after alpha-particle irradiation. *Proc. Natl. Acad. Sci. USA* **95**, 5730–5733 (1998).

14. M. A. Kadhim, D. A. Macdonald, D. T. Goodhead, S. A. Lorimore, S. J. Marsden and E. G. Wright, Transmission of chromosomal instability after plutonium alpha-particle irradiation. *Nature* **355**, 738–740 (1992).

15. L. J. Wu, G. Randers-Pehrson, A. Xu, C. A. Waldren, C. R. Geard, Z. Yu and T. K. Hei, Targeted cytoplasmic irradiation with alpha particles induces mutations in mammalian cells. *Proc. Natl. Acad. Sci. USA* **96**, 4959–4964 (1999).

16. W. E. Wilson, D. J. Lynch, K. Wei and L. A. Braby, Microdosimetry of a 25 keV electron microbeam. *Radiat. Res.* **155**, 89–94 (2001).

17. D. T. Goodhead, J. Thacker and R. Cox, Effectiveness of 0.3 keV carbon ultrasoft X-rays for the inactivation and mutation of cultured mammalian cells. *Int. J. Radiat. Biol.* **36**, 101–114 (1979).

18. K. M. Prise, M. Folkard, S. Davies and B. D. Michael, Measurement of DNA damage and cell killing in Chinese hamster V79 cells irradiated with aluminum characteristic ultrasoft X rays. *Radiat. Res.* **117**, 489–499 (1989).

19. M. R. Raju, S. G. Carpenter, J. J. Chmielewski, M. E. Schillaci, M. E. Wilder, J. P. Freyer, N. F. Johnson, P. L. Schor, R. J. Sebring and D. T. Goodhead, Radiobiology of ultrasoft X rays. I. Cultured hamster cells (V79). *Radiat. Res.* **110**, 396–412 (1987).

20. S. Griffin, M. A. Hill, D. G. Papworth, K. M. Townsend, J. R. Savage and D. T. Goodhead, Effectiveness of 0.28 keV carbon K ultrasoft X-rays at producing simple and complex chromosome exchanges in human fibroblasts in vitro detected using FISH. *Int. J. Radiat. Biol.* **73**, 591–598 (1998).

21. M. E. Schillaci, S. Carpenter, M. R. Raju, R. J. Sebring, M. E. Wilder

and D. T. Goodhead, Radiobiology of ultrasoft X rays. II. Cultured C3H mouse cells (10T1/2). *Radiat. Res.* **118**, 83–92 (1989).

22. M. N. Cornforth, M. E. Schillaci, D. T. Goodhead, S. G. Carpenter, M. E. Wilder, R. J. Sebring and M. R. Raju, Radiobiology of ultrasoft X rays. III. Normal human fibroblasts and the significance of terminal track structure in cell inactivation. *Radiat. Res.* **119**, 511–522 (1989).

23. S. Carpenter, M. N. Cornforth, W. F. Harvey, M. R. Raju, M. E. Schillaci, M. E. Wilder and D. T. Goodhead, Radiobiology of ultra-soft X rays. IV. Flat and round-shaped hamster cells (CHO-10B, HS-23). *Radiat. Res.* **119**, 523–533 (1989).

24. G. Schmahl, D. Rudolph, B. Niemann and O. Christ, Zone-plate X-ray microscopy. *Q. Rev. Biophys.* **13**, 297–315 (1980).

25. S. Peng, M. Folkard, S. Gilchrist, R. J. Locke, Z. Yu and B. D. Michael, Measurements of the targeting accuracy of the Gray Laboratory charged-particle microbeam. *Nucl. Instrum. Methods*, in press.